New Results from the Silicon Vertex Detector of the Belle II Experiment

L. Corona^{a,b,*}, **K. Adamczyk**^{c}, **L. Aggarwal**^{d}, **H. Aihara**^{e}, **T. Aziz**^{f}, **S. Bacher**^{c},
S. Bahinipati^g, **G. Batignani**^{a,b}, **J. Baudot**^{h}, **P. K. Behera**^{i}, **S. Bettarini**^{a,b}, **T. Bilka**^{j},
A. Bozek^c, **F. Buchsteiner**^{k}, **G. Casarosa**^{a,b}, **T. Czank**^{l}, **S. B. Das**^{m}, **G. Dujany**^{h},
F. Forti^{a,b}, **M. Friedl**^{k}, **A. Gabrielli**^{n,o}, **E. Ganiev**^{n,o}, **B. Gobbo**^{o}, **S. Halder**^{f}, **K. Hara**^{p,q},
S. Hazra^f, **T. Higuchi**^{l}, **C. Irmler**^{k}, **A. Ishikawa**^{p,q}, **H. B. Jeon**^{r}, **Y. Jin**^{o}, **C. Joo**^{l},
M. Kaleta^c, **A. B. Kaliyar**^{f}, **J. Kandra**^{j}, **K. H. Kang**^{r}, **P. Kapusta**^{c}, **P. Kodyš**^{j},
T. Kohriki^p, **M. Kumar**^{m}, **R. Kumar**^{d}, **C. La Licata**^{l}, **K. Lalwani**^{m}, **S. C. Lee**^{r}, **J. Libby**^{i},
L. Massaccesi^{a,b}, **S. N. Mayekar**^{f}, **G. B. Mohanty**^{f}, **T. Morii**^{l}, **K. R. Nakamura**^{p,q},
Z. Natkaniec^c, **Y. Onuki**^{e}, **W. Ostrowicz**^{c}, **A. Paladino**^{a,b}, **E. Paoloni**^{a,b}, **H. Park**^{r},
G. Polat^s, **K. K. Rao**^{f}, **I. Ripp-Baudot**^{h}, **G. Rizzo**^{a,b}, **D. Sahoo**^{f}, **C. Schwanda**^{k},
J. Serrano^s, **J. Suzuki**^{p}, **S. Tanaka**^{p,q}, **H. Tanigawa**^{e}, **R. Thalmeier**^{k}, **R. Tiwari**^{f},
T. Tsuboyama^{p,q}, **Y. Uematsu**^{e}, **O. Verbycka**^{c}, **L. Vitale**^{n,o}, **K. Wan**^{e}, **Z. Wang**^{e},
J. Webb^t, **J. Wiechczynski**^{b}, **H. Yin**^{k} and **L. Zani**^{s}
(Belle II SVD Collaboration)

^{a}*Dipartimento di Fisica, Università di Pisa,*
I-56127 Pisa, Italy

^{b}*INFN Sezione di Pisa,*
I-56127 Pisa, Italy

^{c}*H. Niewodniczanski Institute of Nuclear Physics,*
Krakow 31-342, Poland

^{d}*Punjab Agricultural University,*
Ludhiana 141004, India

^{e}*Department of Physics, University of Tokyo,*
Tokyo 113-0033, Japan

^{f}*Tata Institute of Fundamental Research,*
Mumbai 400005, India

^{g}*Indian Institute of Technology Bhubaneswar,*
Satya Nagar, India

^{h}*IPHC, UMR 7178, Université de Strasbourg, CNRS,*
67037 Strasbourg, France

^{i}*Indian Institute of Technology Madras, Chennai 600036, India*

^{j}*Faculty of Mathematics and Physics, Charles University,*
121 16 Prague, Czech Republic

*Speaker

[k] *Institute of High Energy Physics, Austrian Academy of Sciences,*
  1050 Vienna, Austria

[l] *Kavli Institute for the Physics and Mathematics of the Universe (WPI), University of Tokyo,*
  Kashiwa 277-8583, Japan

[m] *Malaviya National Institute of Technology,*
  Jaipur 302017, India

[n] *Dipartimento di Fisica, Università di Trieste,*
  I-34127 Trieste, Italy

[o] *INFN Sezione di Trieste,*
  I-34127 Trieste, Italy

[p] *High Energy Accelerator Research Organization (KEK),*
  Tsukuba 305-0801, Japan

[q] *The Graduate University for Advanced Studies (SOKENDAI),*
  Hayama 240-0193, Japan

[r] *Department of Physics, Kyungpook National University,*
  Daegu 41566, Korea

[s] *Aix Marseille Université , CNRS/IN2P3, CPPM,*
  13288 Marseille, France

[t] *School of Physics, University of Melbourne, Melbourne,*
  Victoria 3010, Australia

  E-mail: luigi.corona@pi.infn.it

The Silicon Vertex Detector (SVD) consists of four layers of double-sided silicon strip sensors. The SVD is one of the two vertex subdetectors within Belle II. Since the start of data taking in 2019 at the Super-KEKB collider (KEK, Japan), which has the highest peak-luminosity ever recorded, the SVD is operated reliably and with high efficiency, despite exposure to harsh beam background. Measurements using data show that the SVD has both high signal-to-noise ratio and hit efficiency, as well precise spatial resolution. Further these properties are stable over time. Recently the simulation has been tuned, using data, to improve the agrement between data and MC for cluster properties. The good hit-time resolution can be exploited to further improve the robustness against the higher levels of background expected as the instantaneous luminosity increases in the next years of running. First effects of radiation damage on strip noise, sensor currents and depletion voltage have been measured, although they do not have any detrimental effect on the performance of the detector.

A. Introduction

Belle II [1] is a luminosity-frontier experiment exploring new physics beyond the Standard Model. It operates at the SuperKEKB collider [2], located at the KEK laboratory in Tsukuba, Japan. SuperKEKB is a second generation B-factory that collides 7 GeV e^- and 4 GeV e^+ mostly at the energy in the center of mass frame of 10.58 GeV. SuperKEKB is designed to reach the highest world luminosity of 6.5×10^{35} cm^{-2}s^{-1}, while the target integrated luminosity is 50 ab^{-1}. The experiment with the full detector has been operated since March 2019. Up to now 213 fb^{-1} of data have been collected and SuperKEKB delivered the peak luminosity of 3.12×10^{34} cm^{-2}s^{-1} on June 2021.

Figure 1 shows the cross-section view of the Belle II Vertex Detector (VXD). It consists of the 2-layer Pixel Detector (PXD) made of DEPFET sensors, and the 4-layer Silicon Vertex Detector (SVD) made of ladders with double-sided silicon strip detectors (DSSD). SVD main tasks are: the extrapolation of the reconstructed particle tracks to PXD, the standalone tracking, and the particle identification using the SVD's dE/dx information.
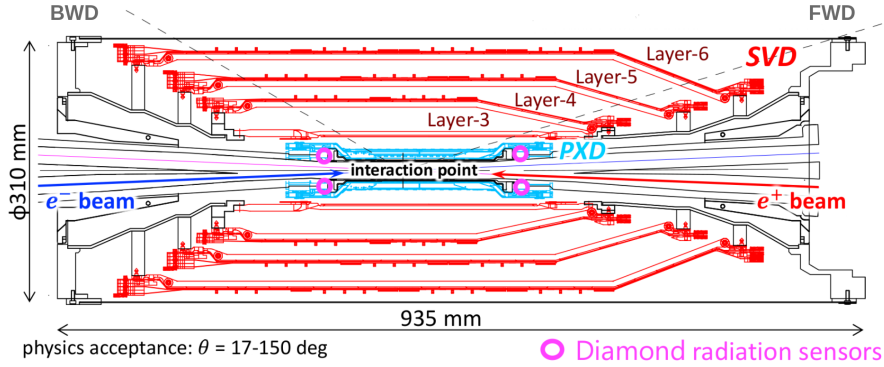
Figure 1: The cross-section view of the VXD: SVD and PXD are represented with red and light blue color, respectively. The pink circles indicate the positions of the diamond sensors installed on the beam pipe.

B. Belle II Silicon Vertex Detector

SVD consists of four layers named layer-3, 4, 5 and 6 from the inner to outer, respectively composed of 7, 10, 12 and 16 ladders with 2, 3, 4 and 5 sensors each. The averaged material budget per layer is 0.7%X_0, where X_0 is the radiation lenght. Additionally, diamond sensors, used both in the beam abort system and to measure the radiation dose on SVD, are installed on the beam pipe [3]. In total, SVD has 172 DSSD sensors, covering a sensible area of 1.2 m^2, with a total of 224k readout strips. The DSSD sensors are fabricated based on the n-type bulk, and they have two sides with p and n doped orthogonal strips, respectively called p- and n-side. The readout strips are AC coupled: the sensing strips are implanted in the n-type bulk and the readout metal strips are placed on top of the implanted strips, separated by a dielectric SiO$_2$. There is a floating strip between two adjacent readout strips on both sides. SVD layer-3 is equipped with only small rectangular sensors, the forward slanted sensors are trapeizoidal and all the remaining are large rectangular sensors. In all sensors, the n-side strips have larger pitches (160 μm for small sensors and 240 μm for large and trapezoidal sensors) compared to the p-side strips (50 μm, 75 μm and 50-75 μm respectively for

small, large and trapezoidal sensors). The number of readout strips on the *p*-side is 768 for all three sensor types. While on the *n*-side, the number of readout strips is 768 for small rectangular sensors and 512 for large rectangular and trapezoidal sensors. Sensor thickness is 320 μm for small and large sensors and 300 μm for trapezoidal sensors. The sensors, with depletion voltage in the range 20-60 V, are operated by applying a bias voltage of 100 V. The SVD front-end readout ASIC is the APV25 chip [4] with 128 input channels, characterized by a short shaping time of 50 ns. It was originally developed for the CMS silicon tracker, and it can tolerate more than 100 Mrad of radiation dose. APV25 chips are operated in multi-peak mode with a clock frequency of 32 MHz. Since the experiment is running at low luminosity and beam background levels, currently 6 subsequent analog samples are recorded to reconstruct the output waveform of each channel. However, in order to reduce bandwidth and data size with increased beam background, the possibility to readout only 3 samples has been studied and can be used.

For the ladder design, SVD adopts the chip-on-sensor concept. It consists of flex circuits directly installed on the sensors, with a thermal isolation foam in between, to reduce the length of the strips and, consequently, the capacitive noise. Moreover, all APV25 chips are installed on the same side of the sensors, and the signal of the strips of the other side is propagated to the APV25 chips thanks to the flex circuits called pitch adapters. This design allows to cool all the sensor chips using only one cooling pipe, reducing the material budget. More details on the ladder design and construction can be found in Reference [5].

## C. SVD operational experience and particle detection performance

SVD was installed in Belle II in November 2018 and has been taking data since March 2019 with smooth and reliable operation. Less than 1% of the total strips in SVD are masked, mainly due to the initial defects caused in the sensor production and a few created in the ladder assembly or developed during the operation. There were a few troubles in the SVD operation so far:

▶ in spring 2019 one APV25 chip in layer-3 was not working properly, so it was disabled and masked in the readout. During summer 2019, the issue was investigated and cured by a cable reconnection. After this incident, all the APV25 chips have been working stably for more than 2.5 years;

▶ in June 2019 a huge beam loss created 10 new pinholes, i.e. the breaking of the AC decoupling capacitor between the implant and the aluminum of the readout strips. While such huge beam losses happened several times after that particular incident, no additional pinholes have been observed so far.

It has been confirmed that SVD performance is excellent by analyzing collision data. In particular, the average sensor hit efficiency is higher than 99.5% stable with time.

To study the cluster charge and signal-to-noise ratio (SNR) distributions, data taken in December 2019 have been used and the results are still valid and shown below. The signal charge released in SVD sensors depends on the track incident angle: indeed the energy deposition scales as $E \sim d/cos\theta$, where d is the sensor thickness and θ is the incident angle. Figure 2a shows the distribution of the signal charge normalized with the track path length and scaled to the sensor thickness of 320 μm for both *p*- (red) and *n*-side (blue) of one backward sensor of layer-3. The fit with the Landau distribution of the normalized charge distribution for the *p*-side returns a most

probable value (MPV) of 21 ke^-. Accounting for a ~15% of uncertainty, it is in agreement with 24 ke^- expected for a minimum ionizing particle (MIP) signal in the 320 μm thickness sensor. Moreover, the *n*-side charge distribution shows a MPV of ~12% smaller than the *p*-side. It is due to the combined effect of the floating strips and the wider strip pitch in the *n*-side than the *p*-side that produces a larger capacitive coupling that causes a signal loss of about 10%-30% in the *n*-side.

(a) Normalized cluster charge.

(b) Cluster signal-to-noise ratio.
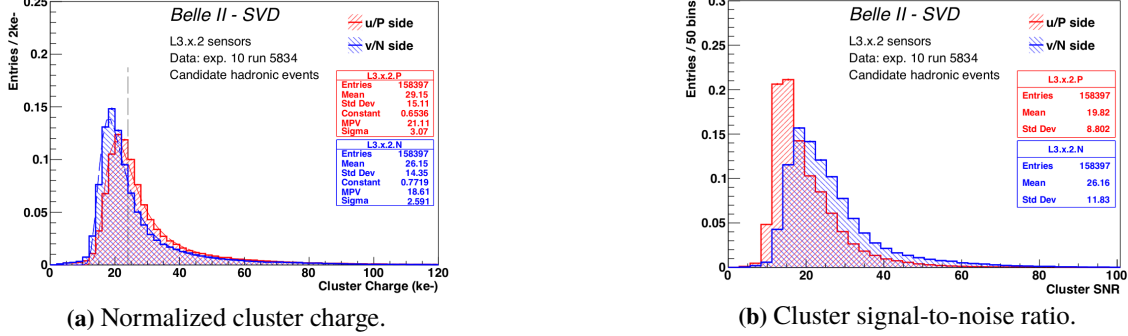
Figure 2: Distributions of the cluster charge normalized with the track path length and scaled to the sensor thickness 320 μm (a) and the cluster signal-to-noise ratio (b) of one sensor in layer-3. The red and blue distributions correspond to the *p*- and *n*-side, respectively. The dashed grey line in correspondence of 24 ke^- in plot (a) represents the expected most probable value of the MIP.

The cluster SNR allows to distinguish the signal clusters from the electrical noise fluctuations. It is defined as the total charge collected in the cluster divided by the square root of the quadratic sum of the noises of the strips associated with the cluster. The cluster SNR distributions for both sensor sides are shown in Figure 2b. Being the strip noise in the *p*-side (740-960 e^-) larger than that in the *n*-side (510-680 e^-), because of the longer strip length and the smaller strip pitch, the MPV of the SNR distribution in the *p*-side is smaller than in the *n*-side. The resulting MPV of the SNR distribution in all 172 sensors ranges from 13 to 30 depending on the sensor side and location.

The hit position resolution depends on the incident angle of the particle trajectory projected to the plane perpendicular to the strip direction (α). The measured resolution in layer-3, which has the finest strip pitches, is 10-15 μm in the *p*-side and 15-30 μm in the *n*-side for $\alpha < 40^o$.

The cluster hit-time is calculated using the hit information of the APV25 samples. The hit-time resolutions are measured from the residuals of the calculated SVD hit-time with respect to the event time evaluated by other detectors with a good time resolution (~ 0.7 ns). The measured SVD hit-time resolutions are 2.9 ns for the *p*-side and 2.4 ns for the *n*-side of layer-3. Currently SVD is running at low background levels, however, with increased beam background, the hit-time information will be crucial to reject off-time beam background hits. Preliminary studies performed on data show we can reject 45% of background cluster keeping a signal efficiency of 99.5%.

D. Beam background and radiation effects on SVD

In general, the beam background produces radiation damage in the sensors and electronics and increases the SVD occupancy, which is also used to monitor the beam background rate. Moreover, larger background occupancy degrades the tracking performance, because it increases the number

of clusters that can be erroneously associated to the track or create fake tracks in the reconstruction. Therefore, it is is important to study how the effect of the beam background amount on SVD evolves. At present time, the limit of the hit occupancy is ~2-3% in layer-3, set by the tracking perfomance studies. However, the preliminary studies on background rejection based on the hit-time selection show that the limit can be relaxed by a factor of ~2. During the operation in summer 2021, the averaged hit occupancy in layer-3 sensors was less than 0.5%, which is well below the present limit.

The projection of the hit occupancy at the original designed luminosity (8×10^{35} cm^{-2}s^{-1}) is estimated by scaling the Monte-Carlo (MC) simulation result by the data/MC ratio evaluated from dedicated beam background studies performed in 2020. The hit occupancy was measured to be 4.1% for layer-3 and smaller for the other layers. The projected layer-3 occupancy exceeds the present limit, but it is expected to be acceptable once the background rejection based on hit-time cut is integrated. The estimated dose rate and equivalent neutron fluence in layer-3 are respectively ~300 krad/sy and $\sim 6.9 \times 10^{11}$ n$_{eq}$/cm^2/sy (sy = 10^7 s).

The integrated dose in the DSSD sensors is evaluated exploiting the correlation between the measured SVD occupancy and the dose rate measured in the diamond sensors. In particular, the correlation coefficients between the diamond sensors and the SVD hit occupancy in each layer are measured on data as well as conversion factor from the hit occupancy to the dose rate. In this way the SVD dose rate can be estimated even when SVD is not taking data using the diamonds dose rate. From the measured diamond integrated dose in the first 2.5 years of operation, a preliminary estimate of the integrated dose in layer-3 middle plane sensors, where the spatial beam background distribution shows a maximum, results to be 60 krad. Assuming the ratio between dose and 1 MeV equivalent neutron fluence from MC simulation, which is 2.3×10^9 n$_{eq}$/cm^2/krad, the integrated amount of 1 MeV equivalent neutron fluence in layer-3 middle-plane sensors over the 2.5 years of operation is estimated to be 1.4×10^{11} n$_{eq}$/cm^2.

(a) Leakage current vs integrated dose.

(b) Slope distribution.
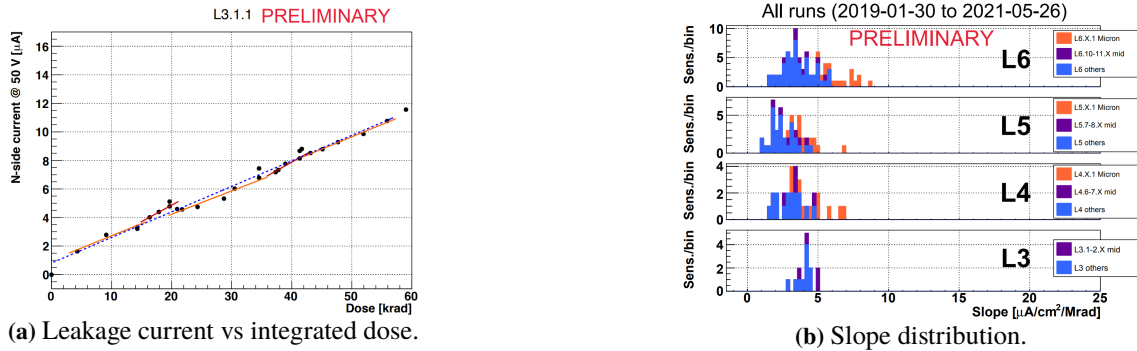
Figure 3: (a) Leakage current in one forward sensor of layer-3 as a function of the integrated dose. The red lines are the linear fitting results for each Belle II operation period, and the blue dotted line is the linear fitting result over 2.5 years of operation. (b) Distributions of slopes of the linear fitting results for all sensors in the four layers.

A visible radiation effect on SVD is the increase of the sensor leakage current. The main causes are the sensor bulk damage and the surface generation current, respectively due to the non-ionizing energy loss and to defects induced by ionizing damage at the interface between the metal strips and the SiO$_2$, although this second contribution is expected to be smaller. The increase of leakage

current due to bulk damage, according to the NIEL hypothesis [6], is proportional to the 1 MeV equivalent neutron fluence, which, in turn, is proportional to the integrated dose, assuming the radiation field due to machine background is not changing with time. This evolution was in fact observed and Figure 3a shows the linear correlation between the leakage current and the integrated dose in one forward sensor of the layer-3. The leakage current increase rate is measured by the slope obtained from the linear fit. Figure 3b shows that the leakage current increase rates in all sensors range from 2 to 5 μA/cm^2/Mrad, which are of the same order measured by BaBar: 1 μA/cm^2/Mrad at 20°C [7]. An averaged dose in each layer is used for all sensors, and the widths of the distributions are due to temperature effects and the dose spread among sensors in the layer. With the short shaping time of the APV25 chips (50 ns) the noise contribution from the leakage current is highly suppressed. With the measured slopes the increase of the leakage current per strip in the layer-3 middle-plane sensors will not affect significantly the total strip noise even after 10 years at design luminosity (corresponding to about 3 Mrad of dose with present background extrapolation), while it will become comparable with present noise after about 10 Mrad.

Another radiation effect is the increase of the strip noise due to the ionizing energy loss in the sensor surface that creates the fixed charge in the SiO$_2$ layer, which increases the inter-strip capacitance. Figure 4 shows the averaged noise as a function of the integrated dose for layer-3 middle-plane sensors (red), the remaining layer-3 sensors (pink), and one middle sensor of layer-4, 5 and 6 (blue, green and black). After the irradiation of 60 krad, the noise is increased of 20-25% in layer-3. The increase of the fixed oxide charge is expected to be saturated at some point, and the saturation is already seen in the *n*-side and starting to be seen in the *p*-side.
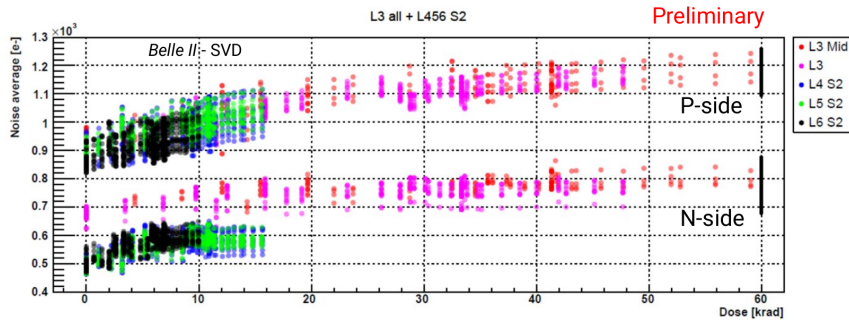
Figure 4: Averaged noise as functions of the integrated dose for layer-3 middle-plane sensors, the remaining layer-3 sensors, and one middle sensor of layer-4, 5 and 6.

The sensor bulk damage due to the non-ionizing energy loss can also change the depletion voltage. Since the substrate of the DSSD sensors is *n*-type, the applied bias voltage develops the sensor depletion from the *p*-side toward the *n*-side. Therefore, the *n*-side strips, are completely insulated when the full depletion is reached, thanks to the *p*-stop implant that interrupts the e^- accumulation layer present in the silicon at the Si-SiO$_2$ interface, so their noise drops to a minimum level. Exploiting this feature, the full depletion voltage has been monitored since July 2020 by measuring the *n*-side strip noise as a function of the bias voltage. No visible change is observed since July 2020 consistently with the very small integrated equivalent neutron fluence expected, which is estimated to be about 1.4×10^{11} n$_{eq}$/cm^2 from the diamond dose measurement, on July 7th 2021.

E. Conclusions

SVD has been taking data in Belle II since March 2019, with smooth and reliable operation since the beginning. Excellent SVD performance have been confirmed on data: the avereged hit efficiency over the four layers is higher than 99.5%, the cluster position resolution is 10-15 µm in the *p*-side and 15-30 µm in the *n*-side with some room for improvement in reconstruction and tuning of simulation. Also, the hit-time resolutions are very good, 2.9 ns for the *p*-side and 2.4 ns for the *n*-side of layer-3. When running at higher luminosity and increased beam background, the hit-time based selection will be crucial to reject off-time background hits to reduce SVD occupancy, and consequently maintain good tracking performance. Currently the SVD occupancy limit set by the tracking performance is 2-3% in layer-3, and preliminary studies show that it will be relaxed by a factor ~2 applying the hit-time based selection. Also, SVD is ready to cope with increased beam background thanks to the 3/6 mixed data acquistion mode of the APV25 implemented to reduce the data size to cope with storage and bandwidth limits.

The integrated dose and equivalent neutron fluence in layer-3 middle-plane sensors in 2.5 years of operation are respectively estimated to be 60 krad and 1.4×10^{11} n_{eq}/cm^2. Up to now, the hit occupancy in the layer-3 is on average below 0.5%, and the effects of the radiation damage on strip noise and sensor leakage current are starting to be seen. They are consistent with the expectation and they are not affecting SVD performance.

Acknowledgments

References

[1] Belle-II collaboration, *Belle II Technical Design Report*, 1011.0352.

[2] Y. Ohnishi et al., *Accelerator design at SuperKEKB*, *PTEP* **2013** (2013) 03A011.

[3] S. Bacher et al., *Performance of the diamond-based beam-loss monitor system of Belle II*, *Nucl. Instrum. Meth. A* **997** (2021) 165157 [2102.04800].

[4] M.J. French et al., *Design and results from the APV25, a deep sub-micron CMOS front-end chip for the CMS tracker*, *Nucl. Instrum. Meth. A* **466** (2001) 359.

[5] Belle-II SVD collaboration, *The Belle II silicon vertex detector assembly and mechanics*, *Nucl. Instrum. Meth. A* **845** (2017) 38.

[6] ROSE collaboration, *Developments for radiation hard silicon detectors by defect engineering - Results by the CERN RD48 (ROSE) Collaboration*, *Nucl. Instrum. Meth. A* **465** (2000) 60.

[7] BaBar collaboration, *The BABAR Detector: Upgrades, Operation and Performance*, *Nucl. Instrum. Meth. A* **729** (2013) 615 [1305.3560].